ISSN No: 2348-4845
International Journal & Magazine of Engineering, Technology, Management and Research
A Peer Reviewed Open Access International Journal

Low Leakage Current and High Efficient Transformerless PV Grid-Connected Inverter

Banoth Suman
M.Tech (PEED),
Arjun College of Technology and Sciences.

T.Rakesh, M.Tech
Assistant Professor,
Arjun College of Technology and Sciences.

ABSTRACT

Low spillage present and high proficiency are two key indexes for transformer less PV framework associated inverter. The transformer less inverter topologies have better productivity thanks than sparing transformer, however their semiconductor gadgets are still on hard-exchanging state at present. As a matter of first importance, a novel zero-current-move (ZCT) idea for the single-stage full-connect transformer less PV network associated inverters is exhibited in this paper. Second, the zero-current turn-off for high-recurrence principle switches of the inverters and the zero-current turn-on for assistant switches included are accomplished by presenting two full tanks. Moreover, a group of ZCT transformer less framework associated inverters with sinusoidal heartbeat width balance is found. Particularly, taking zero-current-move six-switch full-connect topology (ZCT-H6-I) for instance, its operation rule, delicate exchanging conditions, obligation cycle imperatives, and parameter outline method of the resounding tank are investigated in point of interest. At long last, the legitimacy of the ZCT idea is checked by a ZCT-H6-I model appraised at 50 kHz, 1 kW.

Index Terms: ***Grid-connected inverter,resonant tank, trans-former less, zero-current-transition (ZCT).***

I. INTRODUCTION

Transformerless Pv network associated inverters have effectively discovered far reaching application by and by [1], [2].The higher transformation proficiency and lower spillage current are two noteworthy pushing powers in the advancement of the transformer-less matrix associated inverter [3]–[17]. Keeping in mind the end goal to enhance the proficiency of the single-stage transformerless matrix associated inverters, two ways are produced: one is building multi-level circuit structures (chiefly concentrating on five-level topologies [18]–[21]); and the other is utilizing new semiconductor gadgets, for example, SiC-sort or GaN-sort gadgets [22], [23].

The single-stage transformerless multilevel matrix associated inverter has a few benefits, for example, lower voltage stress for force gadget, littler channel size and misfortunes, which is helpful to pick up the productivity. Be that as it may, the control technique is advanced given the issue of voltage unbalance for the force devices,and the corrupted unwavering quality of the inverter. The wide band hole (WBG) semiconductor gadgets will advance the advancement of force hardware and enhance the change proficiency basically. In any case, at present, the manufacturing system of the new materials remains focused still, and the rate of completed items is low. Subsequently, the expense of the inverter with WBG gadgets would be expanded altogether, which is re-verse with the objective of "dollar per watt" beginning establishment cost for PV era framework. Under current innovation back-ground, delicate exchanging procedure is a

ISSN No: 2348-4845
International Journal & Magazine of Engineering, Technology, Management and Research
A Peer Reviewed Open Access International Journal

possible decision to further pick up the transformation effectiveness for the transformer less PV matrix associated inverter. Embracing delicate exchanging strategy can fundamentally lessen or, even dispose of the exchanging misfortunes of Si-semiconductor gadget; at same time, the rising and falling procedures of Si-semiconductor gadget can be mellowed to diminish the voltage and current burdens, and electromagnetic obstruction.

In this way, the exchanging recurrence of the transformerless lattice associated inverter with delicate exchanging strategy can be enormously overhauled. The higher exchanging recurrence is valuable to lessen channel estimate, and to expand power thickness. Along these lines, the inverter expense can be lessened essentially by utilizing delicate exchanging strategy [24], [25].

Delicate exchanging system for dc–ac inverter was initially proposed by Divan [26], which got impressive consideration in the previous decades. When all is said in done, the delicate exchanging dc–ac inverter can be named full connection dc–ac inverter, resounding move dc–ac inverter, and burden thunderous dc–ac inverter, as per their exchanging attributes [27]–[31]. What's more, as indicated by the position of resounding branches or helper branches included the inverter topology, the delicate exchanging topologies can be isolated into dc side sort, and air conditioning side sort. Be that as it may, in a few topologies, for the downsides, for example, high voltage and current anxiety, complex control procedure would happen, which make them troublesome for industry applications [31]. Zero-current-move (ZCT) strategy was at first connected in ac–dc and dc–dc con-verter [32], with the alluring components of heartbeat width regulation (PWM) and zero-current turn-off for high-recurrence switches. Consequently, a basic, proficient ZCT topology for single-stage transformerless PV matrix associated inverter (dc–ac) will be appealing.

At the point when the customary full-connect inverter with unipolar sinusoidal heartbeat width regulation (SPWM) is embraced, the normal mode (CM) spillage current may show up on the parasitic capacitor between the PV cell and the ground, which draws out the wellbeing issue and decreases the effectiveness of the inverter [33]. Keeping in mind the end goal to enhance the normal mode execution of the unipolar SPWM full-connect inverter, a ton of top to bottom exploration ponders, where new freewheeling ways are constructedto separate the PV cluster from the framework in freewheeling period, have been directed in [3]–[9]. A couple measures can be di-vided into air conditioning sidestep [3], [6], [7] and dc sidestep [4], [5], [8], [9], individually. In light of the regular mode proportional model of full-scaffold inverter inferred in [33], it is vital that the capability of the freewheeling way is braced to a half information voltage in the freewheeling time frame, rather than detaching the PV exhibit from the lattice just. Contingent upon this run, the high-recurrence regular mode voltage can be totally dispensed with in the unipolar SPWM full-connect inverter with clasping branch. The topologies in [4], [7], and [8], are consenting to previously mentioned conclusion, yet their cinching capacity are distinctive [8].

The topology proposed in [4], named as initial six-switch full-connect topology (H6-I), and another topology outlined in [6] named as second six-switch full-connect topology (H6-II), in this paper indicates best execution as respects to spillage current concealment in existing topologies of single-stage full-connect transformerless PV network associated inverter [8]. Subsequently, enhancing the change productivity taking into account the topologies with the ideal spillage current concealment execution, can better redesign the records of spillage current and effectiveness.

This paper concentrates on enhancing the transformation productivity of the Transformerless full-connect topologies by utilizing delicate exchanging implies. Initial, a zero-current-move H6-I topology (ZCT-H6-I) is proposed, which is inferred by lessening the changing misfortunes to pick up the

ISSN No: 2348-4845
International Journal & Magazine of Engineering, Technology, Management and Research
A Peer Reviewed Open Access International Journal

transformation effectiveness. Contrasted with hard-exchanging H6-I topology (HS-H6-I), two ZCT full tanks are in parallel added to high-recurrence primary force de-indecencies around, which make the high-recurrence fundamental switches running under zero-current turn-off condition. In the meantime, the additional helper switches can accomplish zero-current turn-on. In the proposed ZCT-H6-I, the capability of freewheeling way can likewise be unreservedly braced amid the freewheeling time frame, so that the normal mode voltage is consistent, which is reasonable for transformerless PV lattice associated applications. At long last, this dad per further develops the ZCT idea into different transformerless full-connect topologies, for example, Heric, H5, and H6-II; here a few commonplace ZCT-full scaffold topologies have been exhibited. Clearly, the delicate exchanging system is a key to pick up the change proficiency and decrease the expense for PV network associated inverters.

This paper is sorted out as takes after. Area II introduces the circuit structure and operation methods of the ZCT-H6-I. The delicate exchanging attributes and outline methodology of the thunderous parameters are exhibited in Section III. Segment IV broadens the ZCT idea into a few ordinary transformerless full-connect topologies. The trial comes about because of a 50-kHz, 1-kW ZCT-H6-I model are given in Section V, and the conclusion is given in Section VI.

II. CIRCUIT STRUCTURE AND OPERATION PRIN--CIPLEOF ZCT-H6-I

A. Circuit Structure of ZCT-H6-I

Keeping in mind the end goal to understand the delicate exchanging operation for the high-recurrence principle switches S5 and S6 in the HS-H6-I topology, the full segments C5a , L5a , C6a , L6a , the helper switches S5a, S6a(including their antiparallel diodes or, body diodes D5a

Fig. 1. Novel ZCT-full bridge transformerless PV grid-connected inverter (a) ZCT-H6-I. (b) Key waveforms.

andD6a), and one helper diode Da are acquainted with structure two full tanks, as appeared in Fig. 1(a), L5a = L6a = Lr , and C5a = C6a = Cr . The line-recurrence full-connect inverter comprises of the switches S1 , S2 , S3 , and S4 ; the inductors L1 , L2, and capacitor C1make up the channel associated with the framework; D7and D8are two or three bracing diodes in the freewheelingperiod. The adjustment example of the ZCT-H6-I is the same with the HS-H6-I topology. This segment concentrates on the operation guideline investigation of the ZCT full tank.

B. Operation Principle Analysis

Before the analysis, the following assumptions are given: 1) All semiconductor devices are ideal switches with antiparallel diodes, and the diodes are additionally perfect diodes without parasitic parameters (this presumption will disregard the opposite recuperation issue); 2) the capacitance Cdc1 and Cdc2 of the dc filterare sufficiently vast to be dealt with as a consistent voltage sources (this suspicion will overlook the dc infusion issue), and the inductance L1 and L2 of the air conditioner channel are sufficiently huge to be dealt with as a steady current sources at the exchanging recurrence scale.

Fig. 1(b) demonstrates the key operation waveforms of the ZCT-H6-I at the exchanging recurrence scale. The clarification of the key waveforms is as per the following: S1,4 , S5,6 , and S5a,6a are the door driving signs of S1 and S4 , S5 and S6, S5a and S6a , individually; iCE5 is the current through the switch S5 ; iD5 is the current throughthe diode D5 reverse; uS5 is the voltage over the switch S5 ; iDS5a is the current through the switch S5a ; iD5a is the current through the diode D5a reverse; uS5a is the voltage over the switch S5a ; iDais the current through the diode Da ; uDais the voltage over the diode Da ; iS1,S 4 and iD3,D2 are the current through the switches S1 and S4 , and the current through the diodes D3 and D2 , separately; iL5a and uC5a are the current through the inductor L5a and the voltage over the capacitor C5a , separately, and ILaand UCaare the pinnacle estimation of resounding inductor and thunderous capacitor, separately; iLis the\ current through the inductor L1 , and IL is its adequacy; in positive half cycle of the

ISSN No: 2348-4845
International Journal & Magazine of Engineering, Technology, Management and Research
A Peer Reviewed Open Access International Journal

framework in current, S1 and S4 are dependably ON, S2 and S3 are constantly OFF; in negative half cycle, S1 and S4are constantly OFF, S2 and S3 are dependably ON. S5 and S6 commutate at the high exchanging recurrence with the same substitution arranges, the helper switches S5a and S6a , individually, commutate with S5 and S6 with a covering time, and the drive rationale timing of all switches is delineated in Fig. 1(b). Clearly, the line-recurrence switches S1 − S4 have a touch of exchanging loss,and most of the exchanging misfortunes disseminate on the highfrequency switches S5 and S6 . One complete exchanging cycle can be separated into nine phases; in light of the closeness, just the exchanging modes in the positive half time of the framework in current are portrayed in point of interest.

Stage 1 [t0 ,t1]: Before t0 , S1 , S4 , S5 , and S6 are ON, and it is in the ordinary force transmission period as the HS-H6-I topology. What's more, the voltage uCaacross the resounding capacitors C5a , and C6a is a consistent quality, uC5a = uC6a = UCa≤ 0.5 UP V (generally, the assistant diode Da and antiparallel diodes D5 andD6 would be forward one-sided to brace the full capacitor voltage to 0.5 UP V). The current iLathrough the thunderous inductors L5a and L6a is zero, iL5a = iL6a = 0; the current through the channel inductors L1 and L2 is IL. At t0 ,S5a and S6a are turned ON under the zero-current condition, because of the thunderous inductors, and the equal circuit is appeared in Fig. 2(a), the reverberation is started. The full inductor streams iL5a and iL6a , individually, start to increment, while the resounding capacitorvoltages uC5a and uC6a , separately, lessen owing tothe thunderous activity. In the meantime, the streams through S5and S6 start to diminish, until it compasses to zero at t1. In thisstage

Stage 2 [t1 ,t2]: Allude to Fig. 2(b). At t1 , the diodes D5 and D6 are forward one-sided, and the streams through the antiparallel diodesD5 andD6 , separately, start to increment contrarily. The full inductor streams iL5a and iL6a ceaselessly increment until they achieve the pinnacle current ILa, separately, at t2; in the meantime, the thunderous capacitor voltages uC5a and uC6a constantly diminish until they achieve zero, individually, at t2. In the previously mentioned two phases,

Stage 3 [t2 ,t3]: Allude to Fig. 2(c). At t2 , the streams over the antiparallel diodes D5 and D6 achieve the pinnacle, and afterward start to diminish, individually, until they achieve zero at t3. In the meantime, the full inductor streams iL5a and iL6a , individually, start to diminish from the pinnacle current ILa, while the thunderous capacitor voltages uC5a and uC6a , separately, start to increment contrarily from zero. In the interim amongst t1 and t3 , the high-recurrence fundamental switches S5 and S6 can be killed under the zero-current condition.

Stage 4 [t3]: Allude to Fig. 2(d). At t3 , the assistant switches S5a and S6a are killed, and the helper diode Da is forward one-sided. Two free full tanks have been joined as one resounding tank, as appeared in Fig. 2(d), the proportionate full inductance L'r= 2Lr , and the identical resounding capacitance C' r = 0.5C in the new thunderous tank. In this stage

Stage 5 [t3 ,t4]: Allude to Fig. 2(e). At t3 , the thunderous inductor streams iL5a = iL6a = IL , and afterward they persistently diminish. The ZCT-H6-I goes into the freewheeling time frame, and the freewheeling ways, separately, are S1 ,IL , D3 and come back to S1 in succession, and S4 , IL , D2 , and come back to S4 in grouping. The thunderous capacitor voltages constantly increment contrarily, individually, until they achieve –UCaat t4. In the meantime, the thunderous inductor streams decline to zero both.

Stage 6[t4 ,t5]: Refer to Fig. 2(f). The ZCT-H6-I goes into the normal freewheeling period. The resonant tank stops resonance,
$iL5a = iL6a = 0$, and $uC5a = uC6a = -UCa$.

ISSN No: 2348-4845
International Journal & Magazine of Engineering, Technology, Management and Research
A Peer Reviewed Open Access International Journal

Stage 7 [t5 ,t6]: Refer to Fig. 2(g). At *t*5 , the high-frequency main switches *S*5 and *S*6 are turned ON; the diodes *D*5*a* and *D*6*a* are forward biased under the effect of the resonant capacitor voltages. The currents across the resonant inductors *L*5*a* and *L*6*a* , respectively, begin to increase from zero until they reach the reverse peak current –*I*Laat *t*6 , while the voltages across the resonant capacitors *C*5*a* and *C*6*a* , respectively, start to increasefrom the negative peak voltage −*UCa*until they reach zero

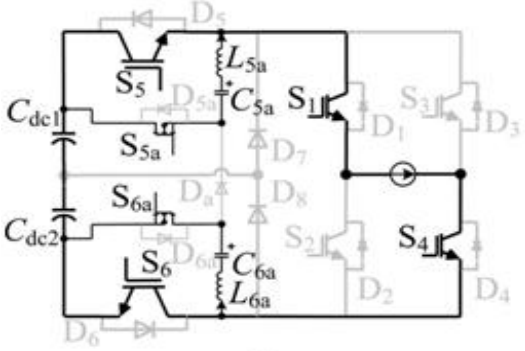

(a)

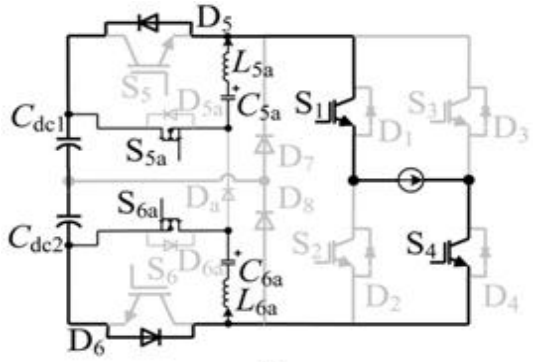

(b)

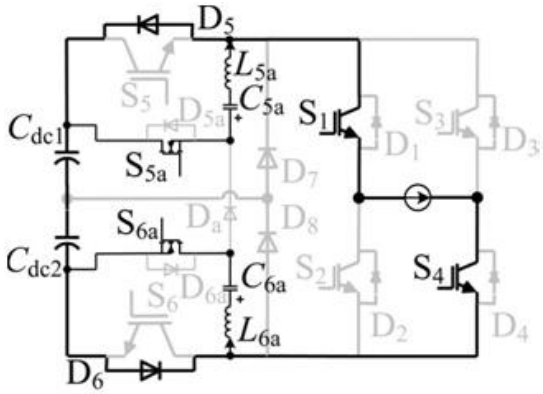

(c)

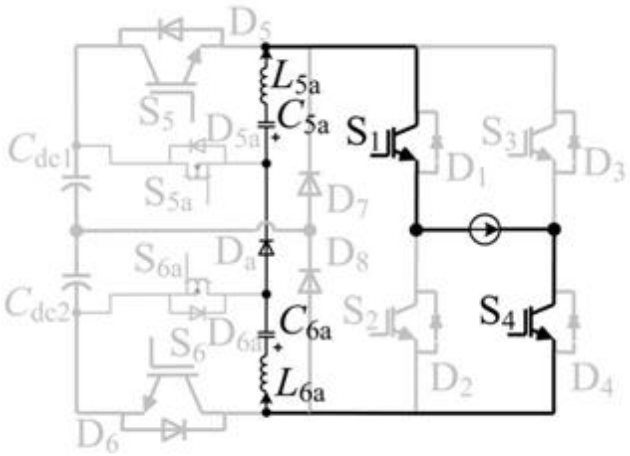

(d)

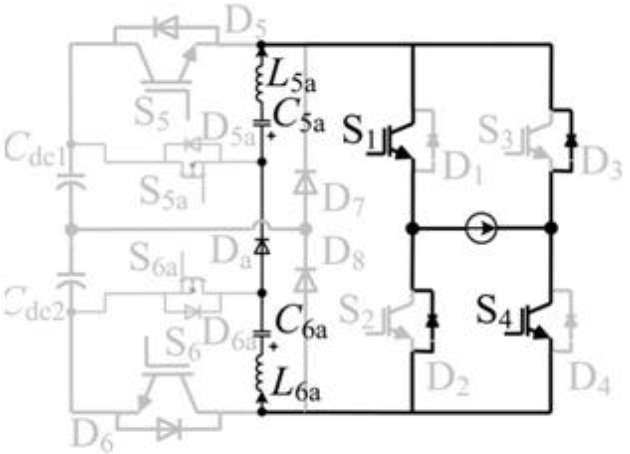

(e)

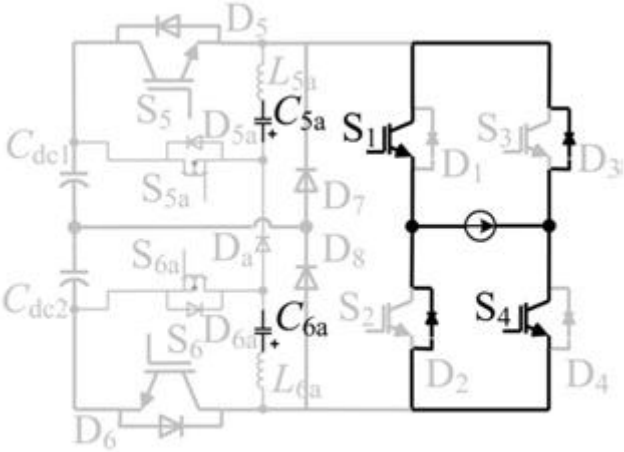

(f)

ISSN No: 2348-4845
International Journal & Magazine of Engineering, Technology, Management and Research
A Peer Reviewed Open Access International Journal

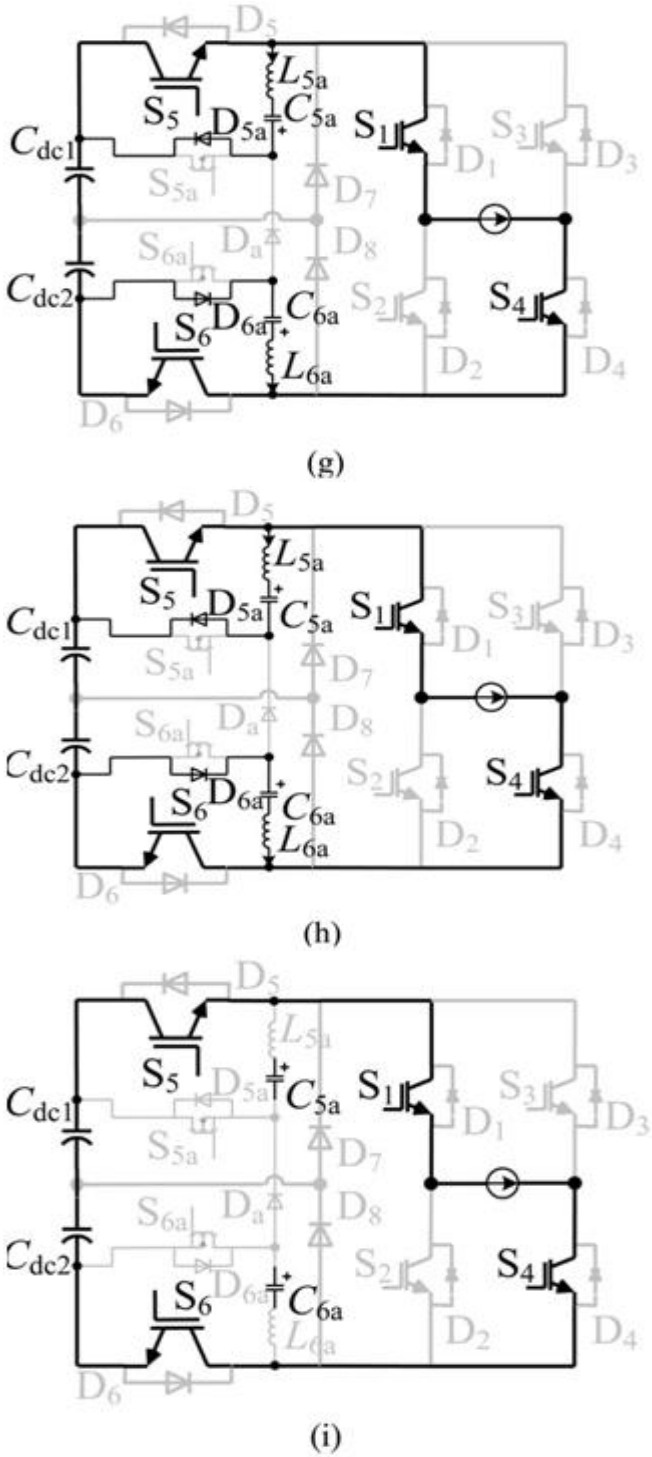

Fig. 2. Equivalent circuits in positive half cycle. (a) Stage 1 [t_0 , t_1], (b) Stage 2 [t_1 , t_2], (c) Stage 3 [t_2 , t_3), (d) Stage 4 [t_3], (e) Stage 5 (t_3 , t_4], (f) Stage 6 [t_4 , t_5], (g) Stage 7 [t_5 , t_6], (h) Stage 8 [t_6 , t_7], and (i) Stage 9 [t_7 , t_8]

Stage 8 [t6 ,t7]: Refer to Fig. 2(h). At *t*6 , the resonant inductor currents *iL*5*a* and *iL*6*a* , respectively, begin to increase from the negative peak current −*I*Launtil they reach to zero at *t*7 ; while the resonant capacitor voltages *uC*5*a* and *uC*6*a* , respectively, increase continually from zero until they reach *UCa*.

Stage 9 [t7 ,t8]: Refer to Fig. 2(i), the ZCT-H6-I works in the normal power transmission period as the H6-I topology. At *t*7 , when the resonant capacitor voltages *uC*5*a* and *uC*6*a* are a constant value *UCa*, and the resonant inductor currents *iL*5*a* and *iL*6*a* are zero, the resonant action stops. At *t*8 , a new switching cycle starts, which is similar with the aforedescribed cycle.

III.Operation Characteristics And Resonant Parameters Design Of Zct-H6-I

A. Achieving Soft-Switching for High-Frequency Main Switches

From Section II, it can be known that in order to achieve

zero-current turn-off for the high-frequency main switches *S*5 and *S*6 , the durations of the stages 2 and 3 must be longer thanthe time of turn-off process of the high-frequency main switches(such as IGBT).Assuming that the high-frequency switches *S*5 and *S*6 are turned OFF at *t*2 , the following equations must be satisfied

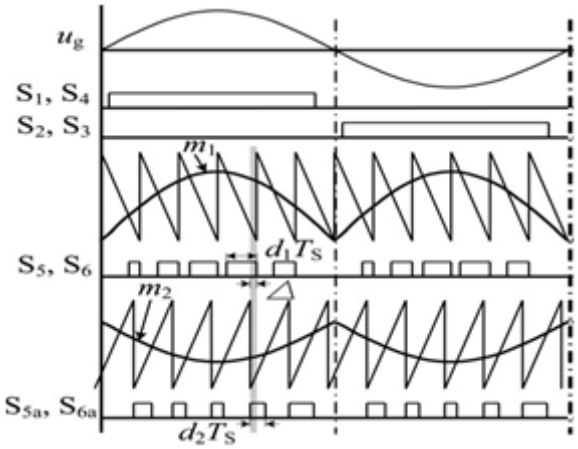

Fig. 3.Generation process of driving signals.

Assuming that d_1 is the duty cycle of the high-frequency main switches S_5 and S_6 , and d_2 is the duty

ISSN No: 2348-4845
International Journal & Magazine of Engineering, Technology, Management and Research
A Peer Reviewed Open Access International Journal

cycle of the helper switches S5a and S6a , as appeared in Fig. 3. Under the conditions that S5 and S6 are killed at t2 , and S5a and S6a are killed at t3 , individually, the covering time of the high-recurrence primary switches and assistant switches is = Tr/4, and the obligation cycle d of the yield differential-mode voltage of the ZCT-H6-I With the suspicions of the matrix in current iL(t) = IREFsinω0 t and the balance signal m = Asin(ω0 t + ϕ) fromthe framework in current controller, themodulation signs of the high recurrence fundamental switches and helper switches can be ascertained where IREF indicates the abundancy of the lattice in current iL, ωo denotes the precise recurrence of the network in current, TS denotesthe exchanging time of the high-recurrence switches and auxiliary switches, and A means the plentifulness of the modulation signal m.

Keeping in mind the end goal to ensure security of the full activity, the planning limitation must be fulfilled as follows:When the ON time d1TS of the high-recurrence fundamental switches is more than a half thunderous cycle (Tr/2), the helper changes are started to work;

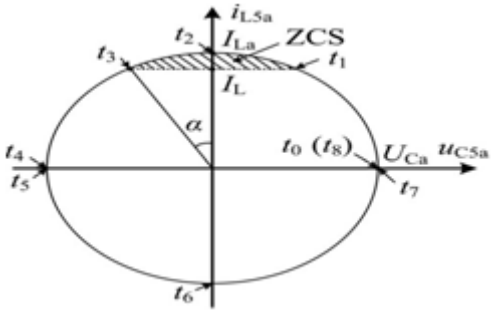

Fig. 4.State-plane trajectory of the resonant action.

Further, the gate driving signals of the high-frequency main switches and auxiliary switches can be generated by comparing the modulation signals *m*1 , and *m*2 with two reverse triangular signals with a phase-shift angle ($2\pi\Delta/TS$), respectively. The process is illustrated in Fig. 3.

C. Parameter Design of Resonant Tank

The design guidelines and steps of the resonant parameters are described as follows:

1. The maximum amplitude *I*Lpof the grid-in current depends on the rated power *PO* of the inverter and the minimum root mean square (rms) voltage *Ug*minof the grid:
2. The peak current I_{La} of the resonant tank depends on the maximum amplitude I_{Lp} of the grid-in current and the angle α, defining $\alpha = 2\pi(t_3-t_2)/T_r$, which is shown in Fig. 4
3. The time t_{off} of the turn-off process of the high-frequency main switches depends on the resonant interval (t_3-t_1):
4. With preselected resonant capacitor voltage U_{Ca} , Z_r can be obtained:

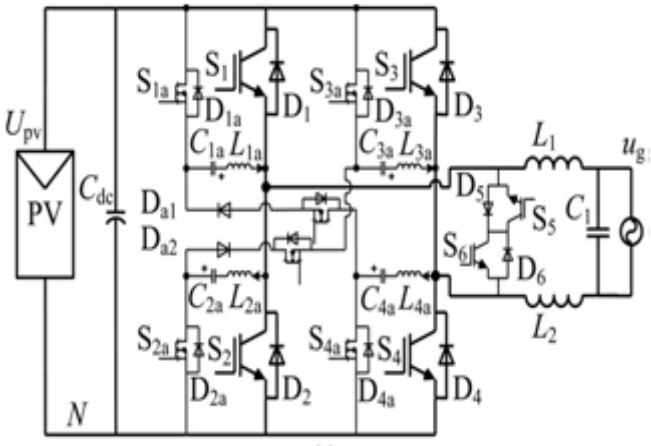

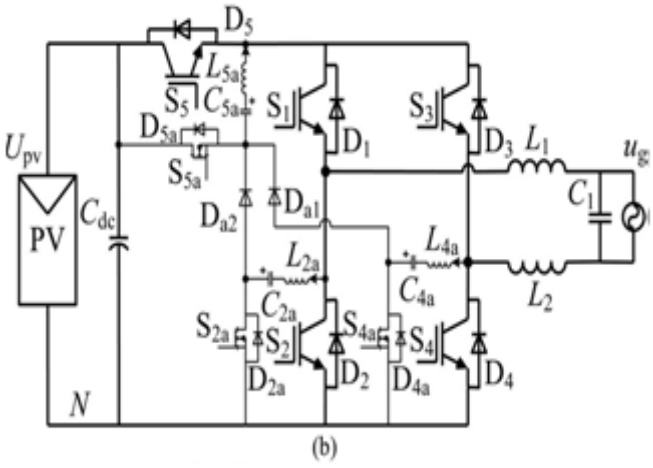

ISSN No: 2348-4845
International Journal & Magazine of Engineering, Technology, Management and Research
A Peer Reviewed Open Access International Journal

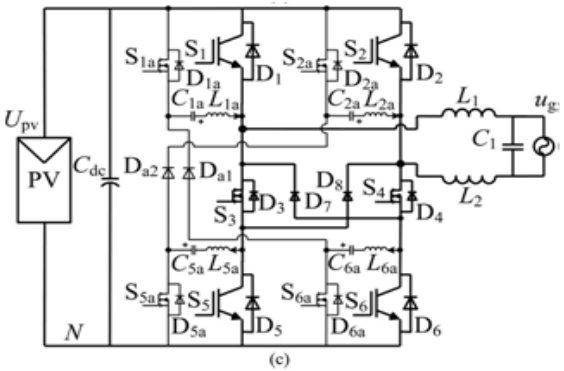

Fig. 5.Family of ZCT-full bridge transformerless PV grid-connected inverters. (a) ZCT-Heric. (b) ZCT-H5. (c) ZCT-H6-II.

at 50 kHz, 1 kW, the parameters of the resonant tank can be cal-culated according to the aforementioned steps. First, the current $I_{L\,p}$can be directly calculated: $I_{L\,p}$= 6.43 *A*. Then, the resonantinductor current $I_{L\,a}$ = 7.43 *A* and T_r = 6 μS can be obtained after choosing the turn-off time t_{off} = 0.5 μS and α = 30°.

Choosing the resonant capacitor voltage $U_{C\,a}$ = 50 V ($\leq U_{pv}/2$ = 200 V), Z_r = 6.73 can be obtained from (21). And then the resonant inductor L_r = 6.5 μH and the resonant capacitor C_r = 140 nF can be derived.

With the selected parameters, the maximum circulating power of the two resonant tanks, which occurs at full load and the lowest input voltage, is about 35 W, which is less than 3.5% of the rated power. Therefore, the size and weight of the introduced

TABLE1
PARAMETERS OF UNIVERSAL PROTOTYPE

Parameter	Value	
	ZCT-H6-I	HS-H6-I
Input voltage [V]	400	
Grid voltage [V]/frequency [Hz]	220/50	
Rated power [W]	1000	
Switching frequency [kHz]	50	
DC-bus capacitor $Cdc1, Cdc2$ [μF]	3×470	
Power device $S1 - -S6$	IKW75N60T	
Power device $S5a, S6a$	FCH47N60F	None
Diode D_a	APT60DQ60B	None
Resonant inductors $L5a, L6a$ [μH]	6.5	None
Resonant capacitors $C5a, C6a$ [nF]	140	None
Filter inductors $L1, L2$ [mH]	0.5	
Filter capacitor C1 [μF]	2	

resonant tanks are ignorable compared with the volume of the HS-H6-I circuit.

IV.FAMILYOFZCTTRANSFORMERLESSFULL BRIDGE TOPOLOGIES

By analyzing the operation principle of the ZCT-H6-I, the characteristics of the resonant tank can be concluded as follows: During the switching transition, the shunt resonant network is activated to create a partial resonance to achieve zero-current turn-off for the high-frequency main switches; when the switching transition is over, the circuit simply reverts back to the familiar PWM operation mode. In this way, the inverter can achieve soft-switching while preserving the advantages of the PWM style. The ZCT concept, illustrated in the ZVT-H6-I in-verter, can also be extended to other transformerless full-bridge grid-connected inverter topologies, such as Heric, H5, and H6-II. Fig. 5 shows several typical ZCT-full bridge transformer-less topologies.

As the descriptions mentioned afore, the added resonant tanks work synchronously with own high-frequency main switches. Especially, the resonant tanks have no effect on the modulation style of the main switches, and the operation principle of the resonant tanks is similar with the ZCT-H6-I.

V. EXPERIMENTAL RESULTS AND DISCUSSIONS

Keeping in mind the end goal to confirm the operation standard and legitimacy of the ZCT idea, a 50-kHz, 1-kW ZCT-H6-I model has been inherent our research facility. The determinations of the model are recorded in Table I.

The test waveforms of the entryway driving signs of the ZCT-H6-I are appeared in Fig. 6, where uG E1 is the door driving voltage of the line-recurrence switch S1 ,uG E5 is the entryway driving voltage of the high-recurrence primary switch S5 , and uG S5a is the door driving voltage of the helper switch S5a . It can be seen that the blanking time of uG S5a is longer than

ISSN No: 2348-4845
International Journal & Magazine of Engineering, Technology, Management and Research
A Peer Reviewed Open Access International Journal

uG E5 's in the zero-intersection time frame, which is in concurrence with the limitation in (17).

The exploratory waveforms of the differential-mode burn acteristics are appeared in Fig. 7 with the predetermined parameters

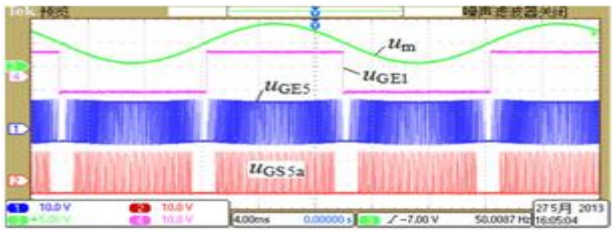

Fig. 6. Experimental waveforms of the modulation and driving signals (*um* :5 V/div, *u*GE1 , *u*GE5, and *u*GS5a : 10 V/div, and time: 4 ms/div).

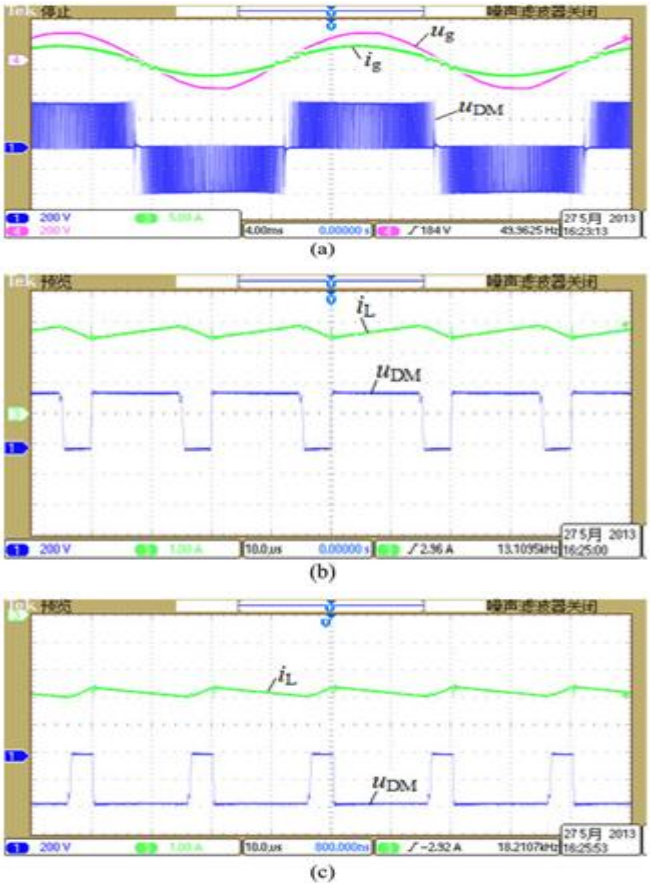

Fig. 7.Experimental waveforms of the matrix voltage, the network in current, and the differential-mode voltage. (a) Differential-mode voltage at the framework recurrence scale (ug and uDM : 200 V/div, ig : 5 A/div, and time: 4 ms/div). (b) Differential-mode voltage in the matrix in current positive half cycle at the exchanging recurrence scale (ig : 1 A/div, and time: 10 µs/div). (c) Differential-mode voltage in negative.

half cycle at the exchanging recurrence scale.of Table I. Fig. 7(a) demonstrates the trial waveforms of the lattice voltage ug , the framework in current ig , and the differential-mode voltage uD M at the network recurrence scale, separately. It can be seen that the differential-mode voltage is of unipolar balance style. Fig. 7(b) and (c) demonstrate the trial waveforms of uD M

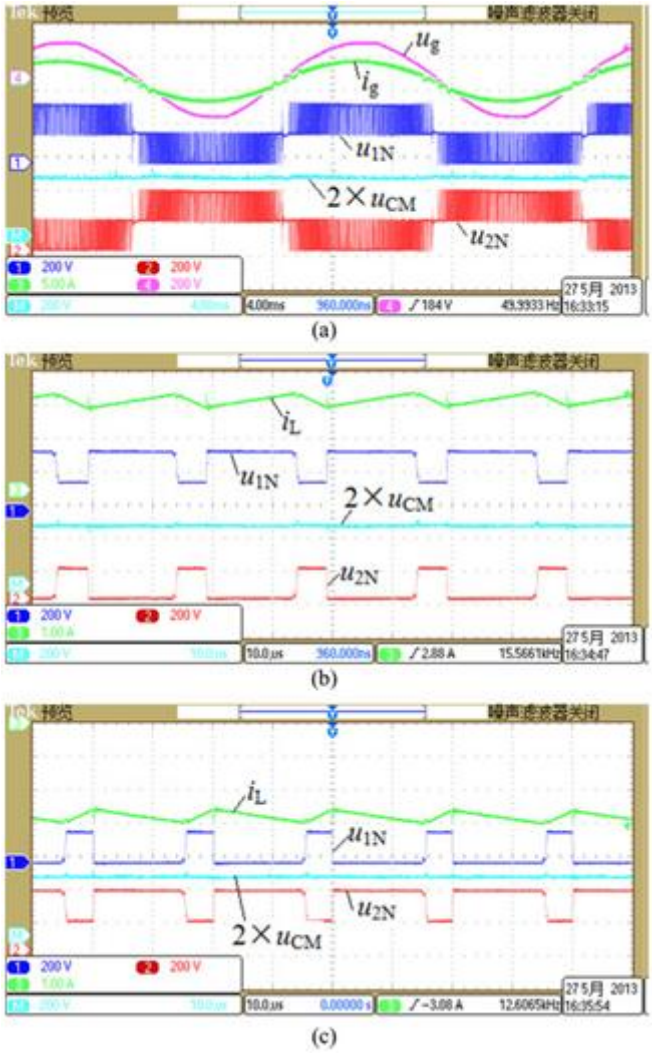

Fig. 8. Test waveforms of the lattice voltage, the framework in current, and normal mode voltage. (a) Common-mode voltage at the matrix recurrence

ISSN No: 2348-4845
International Journal & Magazine of Engineering, Technology, Management and Research
A Peer Reviewed Open Access International Journal

scale (ug,u1N , u2N , and uCM: 200 V/div, ig: 5 A/div, and time: 4 ms/div). (b) Common-mode voltage in positive half cycle at the exchanging recurrence scale (ig: 1 A/div, and time: 10 µs/div). (c) Common-mode voltage in negative half cycle of the network at the exchanging recurrence scale.and the channel inductor current iL at the lattice recurrence scale in the positive half cycle and negative half cycle of the framework in current, individually.

The exploratory waveforms of the basic mode character-istics of the ZCT-H6-I are appeared in Fig. 8. A tenet is finished up in [33], that the spillage current of a full-connect transformer-less inverter relies on upon the adequacy and recurrence of the normal mode voltage under the state of channel inductor symmetric arrangement in stage line and nonpartisan line. Obviously,the regular mode voltage uCM+ u2N) is a consistent quality in Fig. 8(a), and the ZCT full tanks have no impact on the basic mode attributes of ZCT-H6-I contrasted and HS-H6-I. Fig. 7(b) and (c) indicates iL , the voltage u1Nof midpoint 1 to terminal N, the voltage u2Nof midpoint2 to terminal N, and uC M at the exchanging recurrence scale in the positive and negative half time of the framework in current, separately. It can be seen that in the exchanging procedures of turn-on and turn-off, the basic mode voltage is successfully.

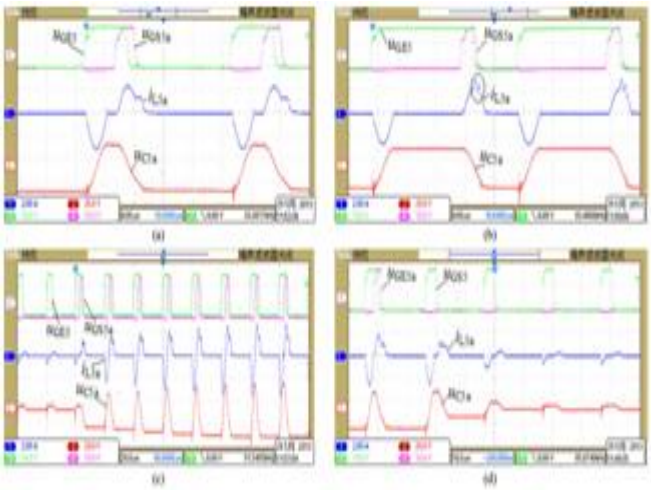

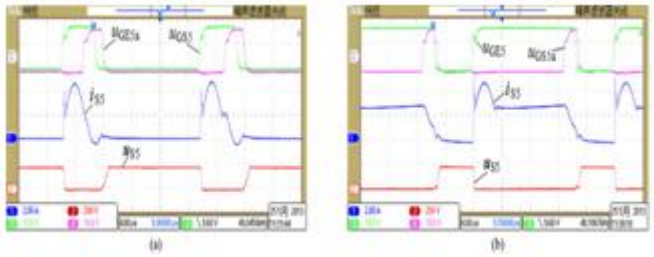

Fig. 9.Experimental waveforms of the resonant tank. (a) In the vicinal of the grid current zero-crossing (u_{GE5} and u_{GS5a} : 10 V/div, u_{C5a} : 100 V/div, i_{L5a} : 2 A/div, and time: 4 μs/div). (b) At the peak of the grid current. (c) Start-resonant process (time: 20 μs/div). (d) Stop-resonant process.

clasped by the latent diodes D7 and D8 . The normal mode normal for the ZCT-H6-I is amazing as HS-H6-I topol-ogy. The test results are well in concurrence with the hypothetical investigation. Consequently, the proposed ZCT-H6-I has the unipolar SPWM differential-mode attributes and the con-stant basic mode execution, which is appropriate for trans-formerless PV framework associated applications.

The trial waveforms of the resounding tank are indicated is Fig. 9(a) and (b) show uG E5 , uG S5a , the resounding current iL5a, and the full voltageuC5aat two diverse obligation cy-cles, separately. Perceptible, when the obligation cycle of the high-recurrence primary changes is near 1, a semi ZCT state may happen contingent upon the measure of capacity vitality of the res-onant tank, and the high-recurrence principle switches have been killed before their present reduction to zero. Under this con-dition, the thunderous way is that from Cdc1→S5a→C5a→L5a → S1 → S4 → L6a → C6a → S6a → Cdc2, and come back to Cdc1in arrangement in Stage 3[t2, t3). The comparable capac-itance of the new full tank is diminished essentially, so that the new thunderous recurrence increments, as appeared operating at a profit circle of Fig. 9(b). This new thunderous tank will hold in Stage 4 until the assistant switches turn-off. Fig. 9(c) and (d) demonstrates the begin full and stop-resounding procedures of the thunderous tank, individually.

ISSN No: 2348-4845
International Journal & Magazine of Engineering, Technology, Management and Research
A Peer Reviewed Open Access International Journal

Clearly, the musical show tion procedure of thunderous tank is security, and the trial waveforms are in concurrence with the hypothetical investigation of Sections II and III.

Fig. 10 demonstrates the trial waveforms of uGE5 ,uG S5a , the go through current iS5 and the collector–emitter voltage uS5of the high-recurrence principle switch S5, separately. It isobvious that before turn-off of S5 , the current iS5 starts to diminish; and when the current iS5 ranges to zero, the antipar-allel diodes D5 is forward one-sided. Along these lines, the zero-current turn-off of S5 is accomplished.

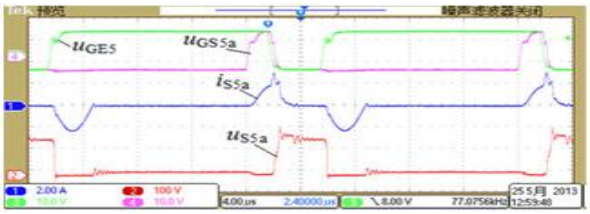

Fig. 11. Experimental waveforms of the auxiliary switch *S5a* (*u*GE5 and*u*GS5a: 10 V/div, *uS5a* : 100 V/div, *iS5a* : 2 A/div, and time: 4 *μ*s/div).

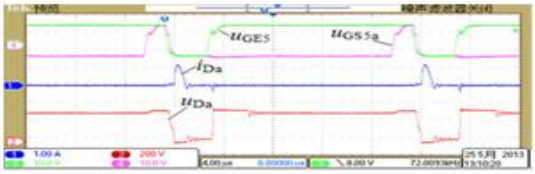

Fig. 12. Experimental waveforms of the auxiliary switch S_{5a} (u_{GE5} and u_{GS5a}: 10 V/div, u_{S5a}: 100 V/div,i_{S5a}: 2 A/div, and time: 4μs/div).

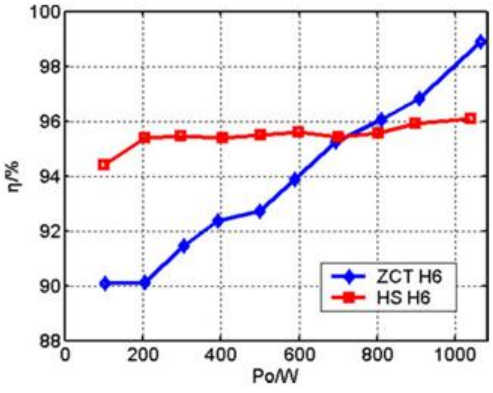

Fig. 13. Efficiency curves comparison between the ZCT-H6-I and HS-H6-I (measured by Digital Power Analyzer VOLTECH PM3300).

Fig. 11 demonstrates the trial waveforms of uGE5 ,uG S5a , the go through current iS5a and the drain–source voltage uS5a of the assistant switch S5a . It can be seen that the turn-on current of S5a is constrained by the resounding inductor L5a , and the zero-current turn-on of the helper switches is accomplished. The exploratory waveforms of the assistant diode Da are appeared in Fig. 12, when the helper switches are killed, the assistant diode is forward one-sided to give the freewheeling way to the resounding current, and this procedure compares to stages 4 and 5 in Section II. The previously mentioned switch operation waveforms are well in concurrence with the hypothetical examination.

Fig. 13 demonstrates the productivity bends of the ZCT-H6-I and HS-H6-I with 50-kHz exchanging recurrence, we can see that the resounding tanks debase the effectiveness in light load because of the course misfortune. In any case, alongside yield power expanding, the effectiveness is enhanced contrasted and HS-H6-I partner. Along these lines, the ZCT innovation is reasonable for higher force rate, for example, higher than 5 kW.

VI. CONCLUSION

The delicate exchanging innovation is essential to push the exchanging recurrence into the larger amount for PV network associated inverter, and the size, weight, and cost can be diminished signif-icantly. A ZCT idea for transformerless full-connect topolo-gies has been proposed in this paper, which has the accompanying qualities. 1) The high-recurrence primary switches acknowledge zero-current turn-off, and the additional assistant switches acknowledge zero-current turn-on. 2) The ZCT full tank has no influ-ence on the differential-mode and basic mode qualities contrasted and hard-exchanging partner.

These benefits are confirmed by a ZCT-H6-I model appraised at 50 kHz, 1 kW. Particularly, the lower proficiency is measured in light load contrasted with HS-H6-I due with the course loss of the additional full tanks; in this way, it can be inferred that the proposed

ISSN No: 2348-4845
International Journal & Magazine of Engineering, Technology, Management and Research
A Peer Reviewed Open Access International Journal

ZCT idea is appropriate for higher force level of single-stage framework associated frameworks with sun oriented cell.

REFERENCES

1. J. M. A. Myrzik and M. Calais, "String and module integrated inverters for single-phase grid connected photovoltaic systems—A review," in Proc.IEEE Bologna Power Tech. Conf., Bologna, Italy, 2003, pp. 430–437.

2. Y. Xue, K. C. Divya, G. Griepentrog, M. Liviu, S. Suresh, and M.Manjrekar, "Towards next generation photovoltaic inverters," in Proc IEEEEnergy Convers. Congr. Expo., 2011, pp. 2467–2474.

3. S. Heribert, S. Christoph, and K. Jurgen, "Inverter for transforming a DC voltage into an AC current or an AC voltage," Europe Patent 1 369 985(A2), May 13, 2003.

4. R. Gonzalez, J. Lopez, P. Sanchis, and L. Marroyo, "Transformerless inverter for single-phase photovoltaic systems," IEEE Trans. Power Elec-tron., vol. 22, no. 2, pp. 693–697, Mar. 2007.

5. M. Victor, F. Greizer, S. Bremicker, and U. Hubler," "Method of converting a direct current voltage from a source of direct current voltage, more specifically from a photovoltaic source of direct current voltage, into a alternating current voltage," U.S. Patent 7 411 802, Aug. 12, 2008.

6. W. S. Yu, J.-S. Lai, H. Qian, C. Hutchens, J. H. Zhang, G. Lisi, A. Djabbari, G. Smith, and T. Hegarty, "High-efficiency inverter with H6-type configuration for photovoltaic non-isolated AC module applications," in Proc. IEEE 25th Annu. Appl. Power Electron. Conf. Expo., 2010, pp. 1056–1061.

7. T. Kerekes, R. Teodorescu, P. Rodriguez, and G. Vazquez, "A new high-efficiency single-phase transformerless PV inverter topology," IEEETrans. Ind. Electron., vol. 58, no. 1, pp. 184–191, Jan. 2011.

8. H. F. Xiao, S. J. Xie, C. Yang, and R. H. Huang, "An optimized trans-formerless photovoltaic grid-connected inverter," IEEE Trans. Ind. Elec-tron., vol. 58, no. 5, pp. 1887–1895, May 2011.

9. B. Yang, W. H. Li, Y. J. Gu, W. F. Cui, and X. N. He, "Improved trans-formerless inverter with common-mode leakage current elimination for a photovoltaic grid-connected power system," IEEE Trans. Power Electron., vol. 27, no. 2, pp. 752–762, Feb. 2012.

10. H. F. Xiao and S. J. Xie, "Transformerless split-inductor neutral point clamped three-level PV grid-connected inverter," IEEE Trans. Power Elec-tron., vol. 27, no. 4, pp. 1799–1808, Apr. 2012.

11. J.-M. Shen, H.-L. Jou, and J.-C. Wu, "Novel transformerless grid-connected power converter with negative grounding for photovoltaic generation system," IEEE Trans. Power Electron., vol. 27, no. 4, pp. 1818– 1829, Apr. 2012.